atmosphere

Article

Extreme Precipitation Events Variation and Projection in the Lancang-Mekong River Basin Based on CMIP6 Simulations

Jing Liu [1], Yanli Liu [1,2,3,4,*], Xin Chen [1,5], Jianyun Zhang [1,2,3], Tiesheng Guan [1,2,3], Guoqing Wang [1,2,3], Junliang Jin [1,2,3], Ye Zhang [1] and Liushan Tang [1]

1 State Key Laboratory of Hydrology-Water Resources and Hydraulic Engineering, Nanjing Hydraulic Research Institute, Nanjing 210029, China; m15638228702@163.com (J.L.); 1020205039@tju.edu.cn (X.C.); jyzhang@nhri.cn (J.Z.); tsguan@nhri.cn (T.G.); gqwang@nhri.cn (G.W.); work_yzhang@163.com (Y.Z.); lstang@nhri.cn (L.T.)
2 Yangtze Institute for Conservation and Development, Nanjing 210098, China
3 Research Center for Climate Change of Ministry of Water Resources, Nanjing 210029, China
4 Cooperative Innovation Center for Water Safety and Hydro Science, Hohai University, Nanjing 210098, China
5 School of Civil Engineering, Tianjin University, Tianjin 300072, China
* Correspondence: ylliu@nhri.cn

Abstract: In recent years, global climate change causes more extreme precipitation events in Lancang-Mekong River Basin (Lancang-Mekong Basin). It leads to the increase of rainstorm and flood risk, which poses a threat to the flood control safety of Lancang-Mekong Basin. Based on the precipitation data of four global climate models of CMIP6, this paper selected six indexes, including PRCPTOT and R10, to study the change characteristics of the extreme precipitation indexes in the Lancang-Mekong Basin during 1980–2020 and predicted the development trend of the extreme precipitation indexes in the Lancang-Mekong Basin during 2021–2050. The results show that from 1980 to 2020, the extreme precipitation events in regions I and IV showed an increasing trend, while those in regions II and III showed a decreasing trend. From 2021 to 2050, the extreme precipitation events in all regions of the Lancang-Mekong River show an upward trend, and most indexes increased compared with the historical period. The extreme precipitation indexes in most regions increases the most under the scenario of SSP5-8.5, while the increase is small under the scenario of SSP2-4.5; The six extreme precipitation indexes selected in the paper can better reflect the trend of extreme precipitation events and floods. The trend of extreme precipitation indexes in the Lancang-Mekong River basin in the future is more significant, which indicates that it may be affected more frequently by extreme precipitation events and floods.

Keywords: Lancang-Mekong Basin; CMIP6; extreme precipitation; regional flood control security

check for updates

Citation: Liu, J.; Liu, Y.; Chen, X.; Zhang, J.; Guan, T.; Wang, G.; Jin, J.; Zhang, Y.; Tang, L. Extreme Precipitation Events Variation and Projection in the Lancang-Mekong River Basin Based on CMIP6 Simulations. *Atmosphere* **2023**, *14*, 1350. https://doi.org/10.3390/atmos14091350

Academic Editor: Corene Matyas

Received: 25 July 2023
Revised: 16 August 2023
Accepted: 24 August 2023
Published: 27 August 2023

Copyright: © 2023 by the authors. Licensee MDPI, Basel, Switzerland. This article is an open access article distributed under the terms and conditions of the Creative Commons Attribution (CC BY) license (https://creativecommons.org/licenses/by/4.0/).

1. Introduction

The sixth assessment report (AR6) of the Intergovernmental Panel on Climate Change (IPCC) points out that the global average surface temperature will reach or exceed 1.5 °C in the next 20 years [1–3]. The changes in extreme events are related to the magnitude of global warming, and as global warming intensifies, extreme precipitation events are likely to become stronger and more frequent [4,5]. The flood disasters caused by extreme precipitation events have caused water and power shortages, damaged buildings, and other problems, which has caused huge damage to social development, national economy, and ecological environment. The study of extreme precipitation events has become the focus of today's society [6].

Aiming at the changes of extreme precipitation events, many scholars have carried out a large number of studies with the help of multiple sets of data products and climate model data. Wang and Qian used the daily rainfall data of 738 meteorological stations in China from 1951 to 2004 to analyze the temporal and spatial distribution of extreme precipitation events with different durations and drew the conclusion that with the continuous increase of extreme precipitation events, the average intensity also increased [7]; Kunkel studied the trend of extreme precipitation in North America and found that since the 1930s, the frequency of extreme precipitation events in the United States has increased significantly, while most extreme events in Canada have shown no significant increase [8]. In a study predicting the future trend of extreme precipitation, Ayugi used six extreme precipitation indexes to predict the future change of extreme precipitation in East Africa based on CMIP6 and proved that the Multi-Model Ensemble (MME) of CMIP6 could better describe the spatial distribution of extreme precipitation. The results suggest that extreme precipitation events are likely to intensify in most parts of Uganda and Kenya, while they may weaken in Tanzania [9]; Xu et al. used 11 extreme precipitation indexes based on CMIP6 to study the future changes of extreme precipitation in China. It is predicted that PRCPTOT (annual total wet day precipitation) and RX5day (MAX 5-day precipitation amount) in China will increase significantly in the next century [10]. Through the analysis of the above studies, it is found that extreme precipitation events are mostly analyzed by selecting extreme precipitation indexes. Therefore, this paper analyzes the development and change characteristics of extreme precipitation events in the Lancang-Mekong River Basin in the past and future by selecting multiple extreme precipitation indexes.

As an important platform for discussion and joint construction of the Belt and Road Initiative, Lancang-Mekong River is one of the regions with the greatest development potential in Asia and even the world, but it is also an area with high risk of flood disaster [11–13]. Affected by extreme climatic events in recent years, the frequency of floods in the Lancang-Mekong Basin is gradually increasing, and the population affected by floods is also increasing [14]. Frequent disasters emphasize the grave situation of flood control security in the Lancang-Mekong River region. Therefore, it is very necessary to analyze the change characteristics and the development trend of extreme precipitation events in the Lancang-Mekong River Basin. However, at present, studies on extreme precipitation events in the Lancang-Mekong River Basin mainly focus on the analysis of the change characteristics of historical extreme precipitation or the prediction of the development trend of future extreme precipitation in some regions [15–19]. The research on the change characteristics and development prediction of extreme precipitation events in the whole basin is limited. With the acceleration of globalization, economic and social links among countries are becoming closer, and frequent floods within the region are more likely to spread to multiple countries, causing huge economic losses and population casualties. Flood disaster has become one of the unavoidable problems in the development of the Lancang-Mekong River Basin. Therefore, it is necessary to analyze the historical characteristics of extreme precipitation and predict its future development trend in the Lancang-Mekong River Basin. It is helpful to provide certain scientific guidance for countries along the Lancang-Mekong River. This can help them jointly manage water resources, maintain regional security, and promote economic development.

2. Data and Methods

2.1. Study Area

The Lancang-Mekong River is the largest international river in Southeast Asia, originating from the northeast of Tanggula Mountain in China. Its upper reaches are called the Lancang River in China and Mekong River after its exit. The Lancang-Mekong River flows through China, Myanmar, Laos, Thailand, Cambodia, and Vietnam, ultimately flowing into the South China Sea in the southwest of Ho Chi Minh City, Vietnam. The total length of the main stream of the river is 4880 km, with a total basin area of 81×10^4 km^2. The landform types of the Lancang-Mekong Basin are complex and diverse. The upper reaches of the Lancang-Mekong Basin originate from the Qinghai-Tibet Plateau with many mountains and valleys. Its middle reaches are hilly with rugged terrain, and the downstream is alluvial plain with flat terrain and frequent floods. The Lancang-Mekong Basin spans nearly 13 latitudes from north to south, and its climate types are complex and changeable, covering almost all climate types in the world except tropical desert climate. Considering the complexity of climatic conditions in the Lancang-Mekong Basin, in order to analyze the climate change of the Lancang-Mekong Basin, this paper divides the study area into four regions according to the precipitation of different magnitude (Figure 1). The area from the source of the Lancang River to the Jiuzhou Hydrologic Station is region I; the Jiuzhou Hydrologic Station to Yunjinghong Hydrologic Station is region II; the Yunjinghong Hydrologic Station to the Vientiane Hydrologic Station is region III; and the Vientiane Hydrologic Station and below is region IV. The average annual precipitation of the four regions is 688 mm, 1238 mm, 1532 mm, and 1722 mm, respectively. The division of these regions reflects the spatial differences of meteorological and hydrological characteristics in the Lancang-Mekong River basin and is conducive to the quantitative evaluation of the trend of extreme precipitation events in different regions.

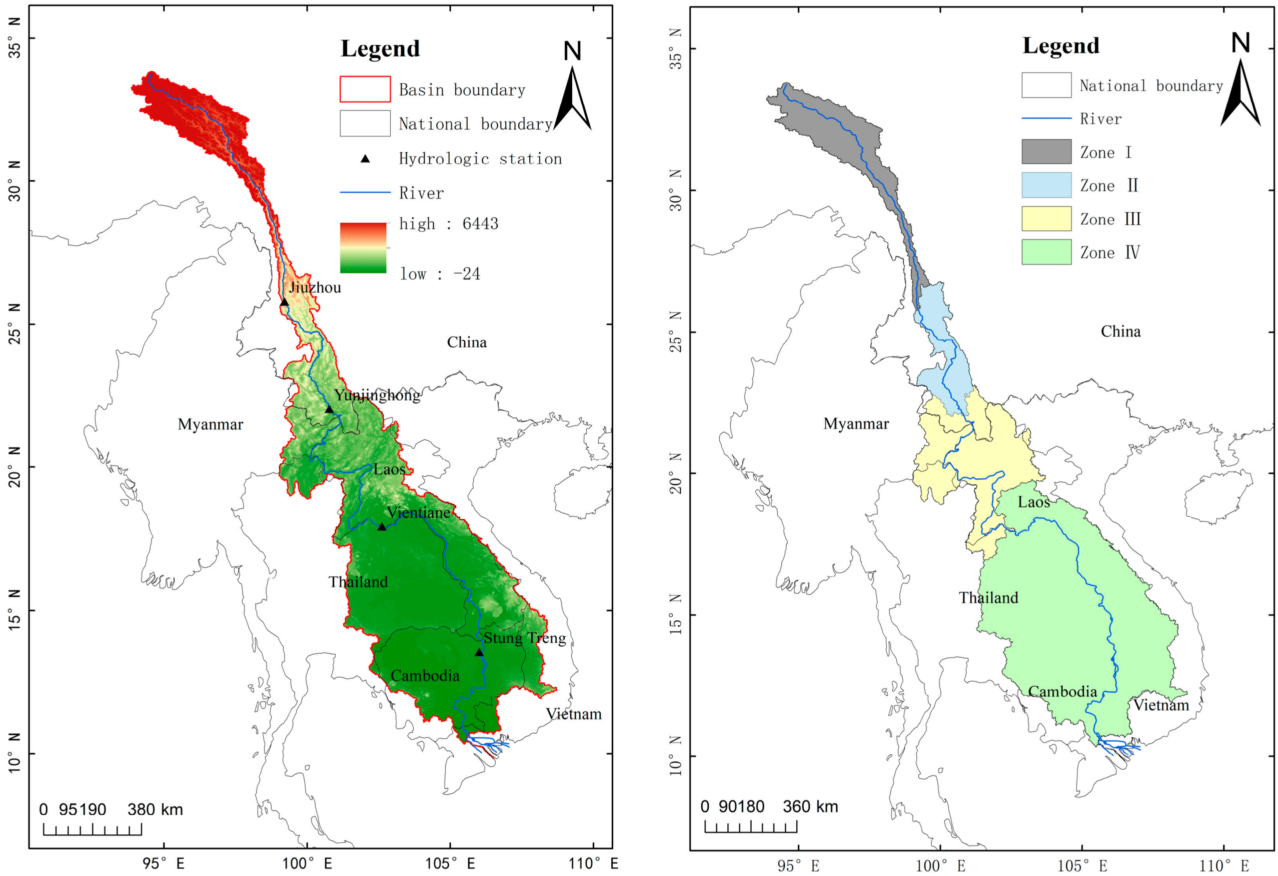

(a) **(b)**

Figure 1. Geographical location and regional division of Lancang-Mekong River Basin. (**a**) Geographical location, (**b**) regional division.

2.2. Data

Precipitation data are derived from the Multi-Source Weighted-Ensemble Precipitation (MSWEP) developed by Beck [20,21], which integrates multiple sets of satellite, measured, and reanalyzed precipitation products. Based on the Budyko framework and global runoff observation, precipitation in regions with complex topography is calibrated with good accuracy [22].

Considering the compatibility between CMIP6 and MSWEP, four global climate models (Table 1) in CMIP6 with good correlation with MSWEP data were selected for daily precipitation grid data. Among the multiple scenarios provided by CMIP6, historical scenarios (1980–2016) and four future climate projections (2021–2050) were selected: SSP1-2.6, SSP2-4.5, SSP3-7.0, SSP5-8.5, representing low, medium, medium to high, and high emission forcing scenarios, respectively [23]. Since the spatial resolution of the four selected climate models is low and different, the bilinear interpolation method is used to unify the spatial resolution to 0.1° × 0.1°, and the Quantile Mapping method is used to correct the deviation of the interpolated mode data on each grid [24].

Table 1. Information of 4 CMIP6 models.

Organization	Country	Mode Name	Mesh Resolution
BCC	China	BCC-CSM2-MR	1.1° × 1.1°
EC-Earth-Cons	Britain	EC-Earth3	0.7° × 0.7°
EC-Earth-Cons	Britain	EC-Earth3-Veg	0.7° × 0.7°
INM	Russia	INM-CM5-0	2.0° × 1.5°

2.3. Methods

2.3.1. Assessment Method of Extreme Precipitation in Watershed

The "Climate Change Monitoring and Indicators" defined by the Expert Team on Climate Change Detection and Indices (ETCCDI) have been widely used in the analysis and study of extreme climate events [25–30]. Considering the geographical location and natural environment characteristics of the study area, six extreme precipitation indexes (Table 2), which are closely related to extreme precipitation events, are selected from the 27 climate indexes of ETCCDI for research. PRCPTOT, R10, R20, R95p, RX5day, and SDII were tested, respectively. These indexes reflect the magnitude and intensity of rainfall, and the simulation effect is good. Linear fitting and the Mann–Kendall mutation test were used to analyze the temporal variation rule and mutation characteristics of the extreme precipitation indexes in the Lancang-Mekong River Basin [31], and the spatial variation of the extreme precipitation indexes in the Lancang-Mekong River Basin is analyzed by using the 10-year sliding average change rate of each extreme precipitation index.

Table 2. Definition of extreme precipitation index.

ID	Indicator Name	Definitions	Units
PRCPTOT	Annual total wet day precipitation	Annual total PRCP in wet days (RR ≥ 1 mm)	mm
R10	Number of heavy precipitation days	Annual count of days when PRCP ≥ 10 mm	days
R20	Number of very heavy precipitation days	Annual count of days when PRCP ≥ 20 mm	days
P95p	Very wet days	Annual total PRCP when RR > 95th percentile	mm
RX5day	MAX 5-day precipitation amount	Maximum consecutive 5-day precipitation	mm
SDII	Simple daily intensity index	Annual total precipitation divided by the number of wet days (defined as PRCP ≥ 1.0 mm) in the year	mm/day

The calculation formula for each extreme precipitation index is as follows:

$$PRCPTOT = \sum_{i=1}^{I} RRi\ (RR_i > 1\ \mathrm{mm}) \tag{1}$$

where I represents the number of rainy days within a year and RR_i represents the daily precipitation on the i-th day.

$$R10 = I_1\ (RR_i \geq 10\ \mathrm{mm}) \tag{2}$$

Among them, RR_i is the daily precipitation on the i-th day of the year. I_1 is the number of days with $RR_i \geq 10$ mm.

$$R20 = I_2 \ (RR_i \geq 20 \text{ mm}) \tag{3}$$

Among them, RR_i is the daily precipitation on the i-th day of the year. I_2 is the number of days with $RR_i \geq 20$ mm.

$$R95p = \sum_{i=1}^{I} RR_i \ (RR_i > RR_{in}95) \tag{4}$$

where RR_i is the daily precipitation, RR_{in} is the 95th percentile of daily precipitation in a year, arranged from high to low, and I represents the number of rainy days in this interval.

$$RX5day = \max(RR_k) \tag{5}$$

Among them, RR_k is the sum of daily precipitation for the 5-day interval ending on the k-th day of the year.

$$\text{SDII} = \frac{\sum_{i=1}^{I} RR_i}{I} \ (RR_i > 1 \text{ mm}) \tag{6}$$

Among them, RR_i is the daily precipitation on rainy days within a year, and I represents the number of days of rainfall.

2.3.2. Uncertainty and Probability Distribution Methods

In response to the uncertainty of CMIP6 single mode estimation, this study applies the Multi-Model Ensemble (MME) to eliminate the influence of the "unicity" and "uncertainty" of CMIP6 single model prediction. MME is a method that utilizes the results of multiple model simulation and further ensemble average to reduce the uncertainty of model simulation, which is widely used in model simulation [32,33]. Therefore, this paper uses CMIP6 precipitation data averaged by Multi-Model Ensemble to predict the development trend of future extreme precipitation events in the Lancang-Mekong Basin.

The Kernel Density Estimation (KDE) in the nonparametric estimation can better fit the probability distribution of extreme precipitation [34,35], so this method is used to estimate the probability distribution of extreme precipitation in the basin under different scenarios. Kernel Density Estimation, also known as Parzen window, is mainly used to estimate the probability distribution of an unknown distribution function by observing its random variable, so as to obtain a smooth sample distribution. For one-dimensional data with n samples, the formula of probability density function obtained by kernel density estimation at point x is:

$$f(x,h) = \frac{1}{nh} \sum_{i=1}^{n} K(\frac{x - x_i}{h}) \tag{7}$$

where: h is bandwidth or window width; K is the kernel.

3. Result

3.1. Historical Extreme Precipitation Events Variation

3.1.1. Temporal Variation of Extreme Precipitation Events

In the historical period, the extreme precipitation indexes in the region from region I and region IV mostly showed an upward trend. In region I (Figure 2), all of the extreme precipitation indexes showed an upward trend, PRCPTOT increased at a rate of 2.630 mm/1a, and the change trend was significant ($p < 0.05$); R10, R20, R95p, RX5day, and SDII all showed a slight increase, but the change trend was not significant ($p > 0.05$). In region IV (Figure 3), four extreme precipitation indexes showed an upward trend, PRCPTOT, R20, R95p, and RX5day increased at a rate of 1.519 mm/1a, 0.032 d/1a, 0.968 mm/1a, and

0.160 mm/1a, respectively. R10 and SDII decreased slowly at the rate of −0.009 d/1a and -0.004 (mm·d^{-1})/1a, respectively, and there were no significant trends in the six extreme precipitation indexes in this region (p > 0.05). However, the extreme precipitation indexes in regions II and region III showed a downward trend, and the downward trend was not significant (p > 0.05).

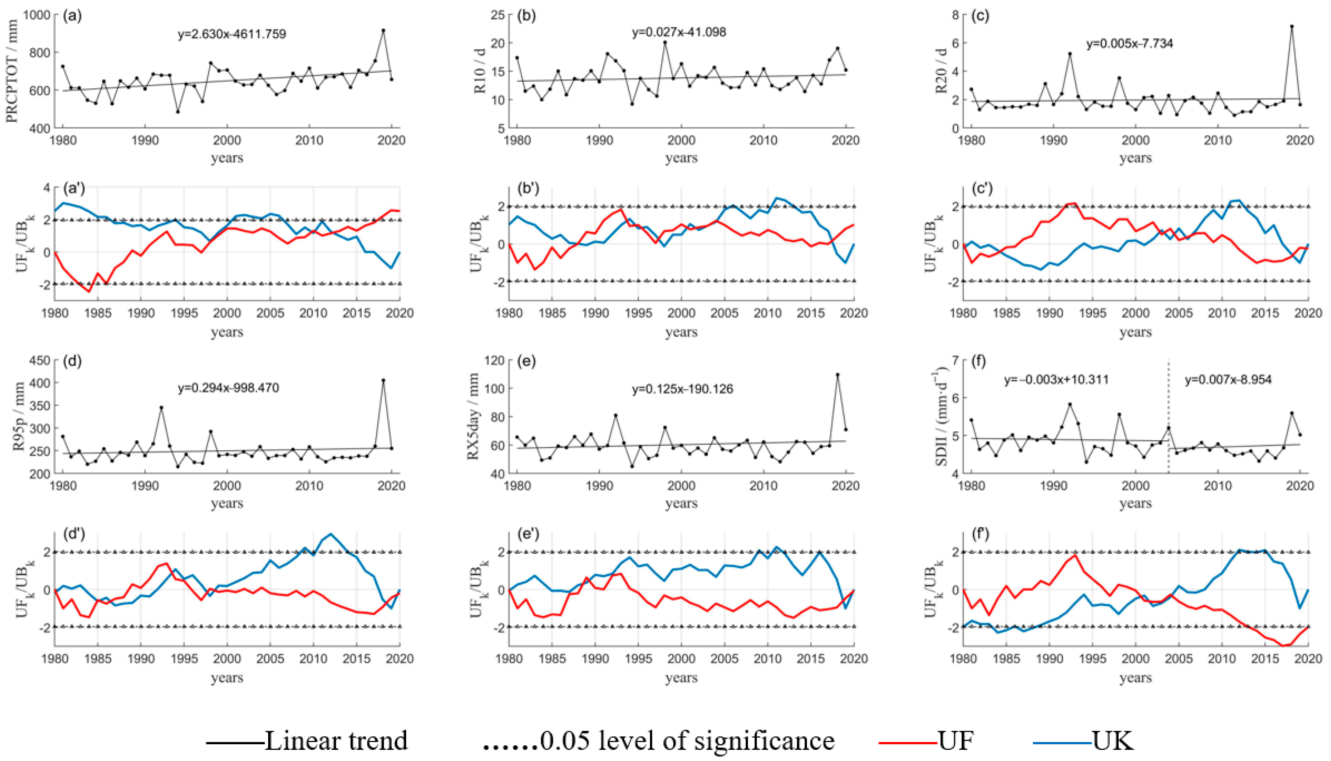

Figure 2. Variation trend and mutation characteristics of extreme precipitation in region I of Lancang-Mekong River Basin from 1980 to 2020. Note: (**a**–**f**) represents the trend of changes in each index, (**a′**–**f′**) represents the mutation characteristics of each index.

From the perspective of the whole basin, the climate status of the Lancang-Mekong Basin was relatively stable during 1980–2020. Among the four sub-regions, only SDII in the region I mutated in 2004, and its change rate changed from −0.003 (mm·d^{-1})/1a to 0.007 (mm·d^{-1})/1a. No significant mutation occurred in other regions. In terms of the possibility of extreme precipitation events, the probability of extreme precipitation events in region II and region III in the past 40 years has decreased gradually, while the probability of extreme precipitation events in region I and region IV has increased gradually.

3.1.2. Spatial Variation of Extreme Precipitation Events

Figure 4 shows the spatial distribution of the change rates of extreme precipitation indexes in the Lancang-Mekong River Basin during 1980–2020. In region I, the change rate of PRCPTOT presented an increasing–decreasing–increasing trend from north to south, and the maximum increase rate is concentrated in the north, about 8~13 mm/10a. The rates of change of R10, R20, and R95p were the same as that of PRCPTOT, and their maximum increase rates were also concentrated in the northern region. The maximum rate of RX5day change was concentrated in the northern part of the country, while the rate of change was unchanged or slightly increased in other regions, and the increase rate was concentrated in the range of 0~3 mm/10a. The maximum change rate of SDII was concentrated in the central and southern regions, and the change rate of other regions was about −0.01~0 (mm·d^{-1})/10a. On the whole, the change rates of the extreme precipitation indexes in this region showed an increasing trend in most areas, and the maximum of the indexes' change rates were mainly concentrated in the northern region, where the terrain was mostly glaciers, bare land, and grasslands. The relief of the terrain became larger and the drainage basin became narrower to the south, and the extreme precipitation would rapidly gather and lead to the occurrence of flood disasters.

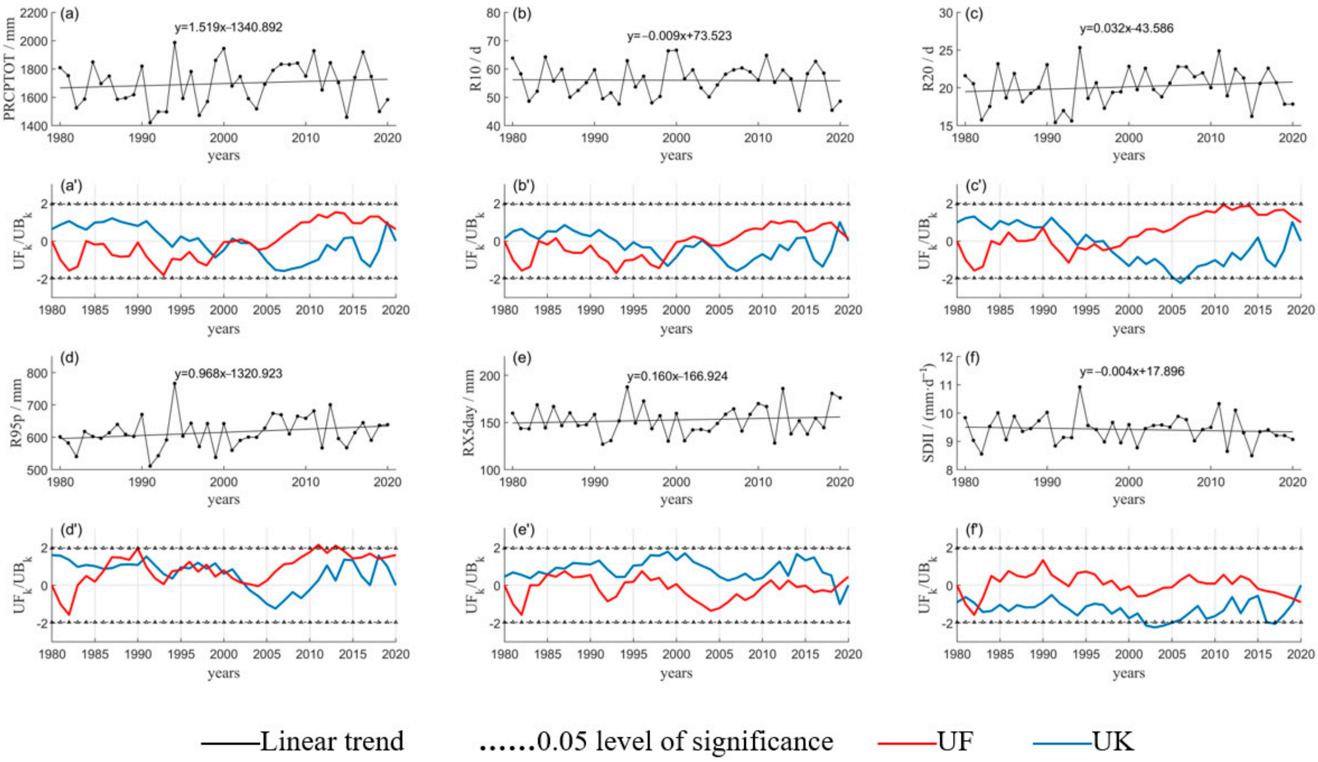

Figure 3. Variation trend and mutation characteristics of extreme precipitation in region IV of Lancang-Mekong River Basin from 1980 to 2020. Note: (**a**–**f**) represents the trend of changes in each index, (**a′**–**f′**) represents the mutation characteristics of each index.

Although the extreme precipitation events in region II and region III showed a decreasing trend on the whole, the extreme precipitation indexes still showed an increasing trend in a few areas. In region II, most of the extreme precipitation indexes followed the increasing–decreasing–increasing–decreasing trend, and the maximum change rates were concentrated in the central region. In the region III, the change rates of most extreme precipitation indexes gradually increased from the middle to the two ends, and the maximum change rates were concentrated in the southern area. Therefore, the middle area of region II and the southern area of region III were still faced with the risk of increasing extreme precipitation events.

In region IV, the distribution patterns of PRCPTOT, R10, R20, R95p, and RX5day change rates were the same, showing obvious zonal differentiation. They showed a decreasing–increasing–decreasing–increasing trend from north to south, and the maximum change rates were concentrated in the central eastern area. The change rate of SDII showed an increasing trend in most regions, with its maximum value appearing in the central northern region and the eastern coastal area, approximately 0.05 (mm·d^{-1})/10a. Region IV is composed of parts of Laos, Thailand, and Cambodia. In addition to large-scale cultivation, the industrial construction in this region is also developed. For example, the Nong Khai and Udon Thani industrial zones in Thailand, the Savannakhet economic park in Laos, and the Phnom Penh economic zone in Cambodia are all located in this region. The intensification of extreme precipitation events would not only inundate crops and damage water conservancy facilities; it would also cause plant equipment damage, preventing normal production, and seriously affect the economic construction and development of the region.

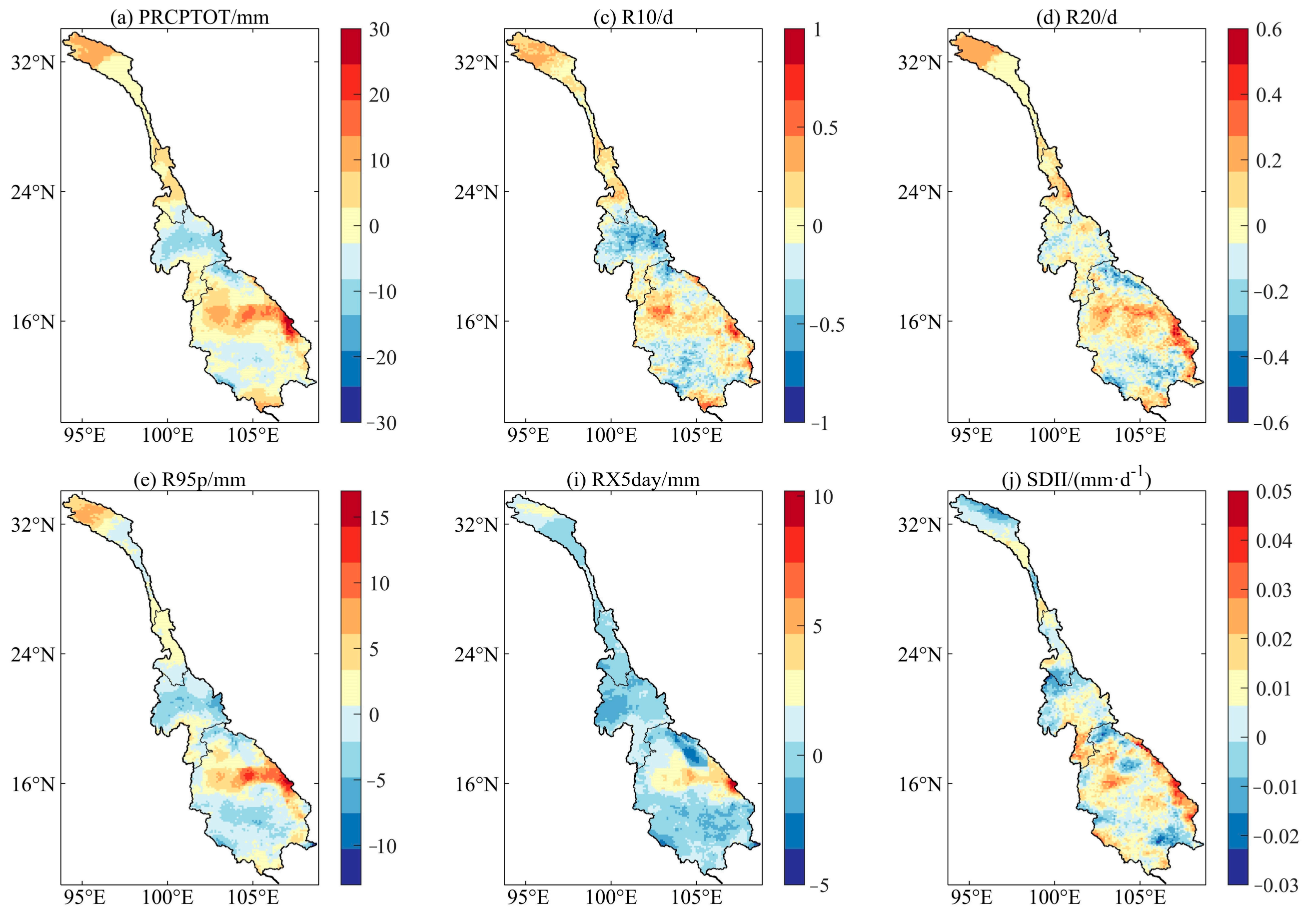

Figure 4. Spatial distribution of extreme precipitation indexes change rates in Lancang—Mekong Basin.

3.1.3. Correlation Analysis of Extreme Precipitation Indexes

In order to verify that the extreme precipitation indexes selected in this paper can better reflect the change trend of extreme precipitation events, this paper defines precipitation events with daily precipitation of 10 mm or above as extreme precipitation events based on different rainfall levels. Figure 5 shows the change trend of the total amount of extreme precipitation events in each region of the Lancang-Mekong Basin from 1980 to 2020. It can be seen from the figure that, extreme precipitation events in region I and region IV showed an upward trend, while those in region II and region III showed a downward trend. The variation trend of extreme precipitation events in each region is the same as that of extreme precipitation indexes. Therefore, the six extreme precipitation indexes selected in this paper are well representative, and the changing trend of extreme precipitation events in each region can be judged according to the changing trend of extreme precipitation indexes.

In addition, Tables 3 and 4, respectively, present statistics for the annual average of extreme precipitation indexes in each region and the extreme precipitation indexes in each region during the occurrence of floods. Affected by heavy rainfall in 1992, 1998, 2001, and 2019, natural disasters such as floods, landslides, and mudslides occurred in many places in Yunnan. Heavy rainfall in southern Thailand in 2011 and central and eastern Thailand in 2013 caused flooding and even minor breakdowns of embankments. By comparing the annual average of extreme precipitation indexes and extreme precipitation indexes in flood years, we can find that: (1) the extreme precipitation indexes increased significantly in flood years. (2) Among six indexes, R20 showed the most significant increase, which was 161.12%, 75.60%, 45.52%, 23.63%, 11.70%, and 257.21% in the year of flood. (3) The increase of R95p and RX5day was also obvious and even exceeded the increase of R20 in Thailand in 2013, reaching 13.86% and 21.84%, respectively. Therefore, the six extreme precipitation indexes selected in this paper can better reflect the occurrence of flood, and the possibility of flood occurrence in a certain region can be judged according to the change of extreme precipitation indexes.

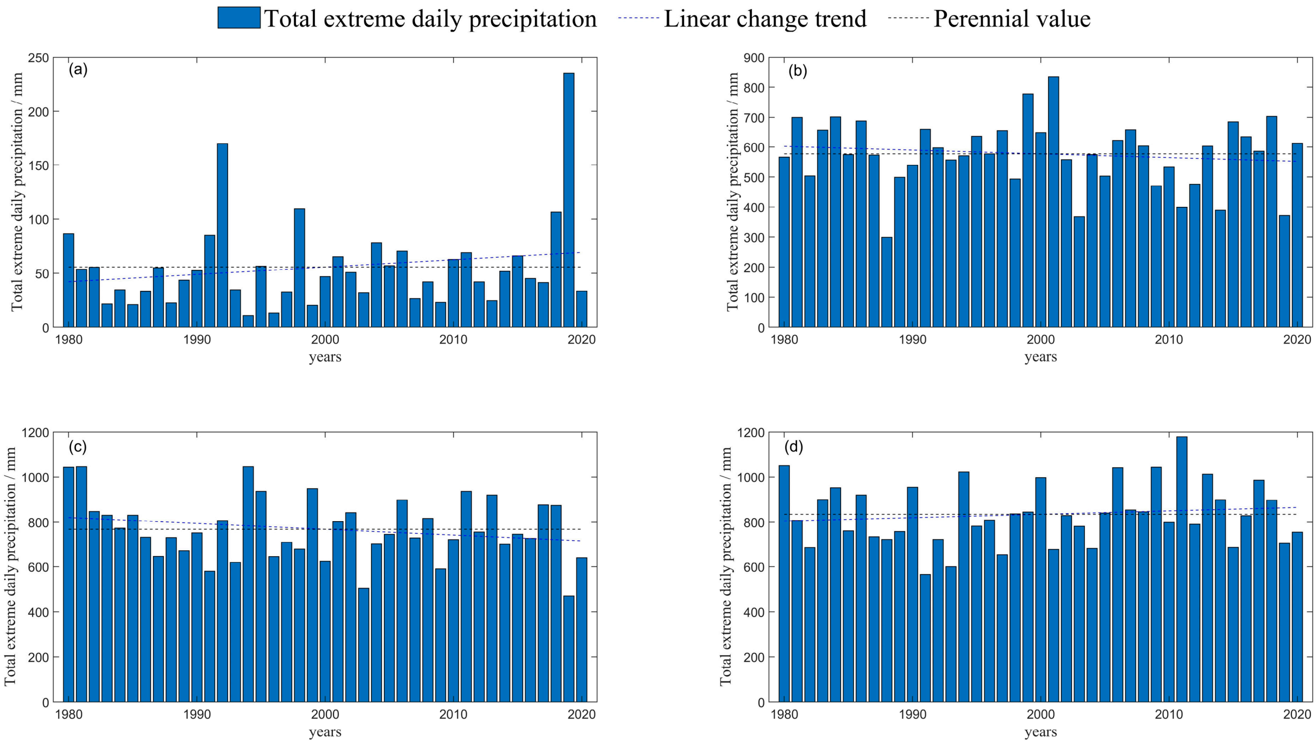

Figure 5. Trends of extreme precipitation events in the Lancang-Mekong River Basin from 1980 to 2020. Note: (**a**–**d**) represent extreme precipitation events in region I to region IV, respectively.

Table 3. Annual average of extreme precipitation index in each region.

Region	PRCPTOT	R10	R20	R95p	RX5day	SDII
I	648.38	14.00	2.00	249.68	60.22	4.81
II	1209.15	39.00	11.00	448.22	106.20	7.44
III	1505.93	50.77	16.64	545.51	130.19	8.67
IV	1696.49	56.00	20.13	615.43	152.66	9.24

Table 4. Flood year and extreme precipitation index.

Year	District	Region	PRCPTOT	R10	R20	R95p	RX5day	SDII
1992	Yunnan	I	677.90	16.80	5.22	344.90	80.88	5.82
1998	Yunnan	I	742.63	20.06	3.51	292.10	72.33	5.56
2011	Yunnan	II	1413.57	49.42	16.00	498.54	109.77	8.09
2011	Thailand	IV	1928.48	64.79	24.89	681.60	166.92	10.33
2013	Thailand	IV	1843.73	59.60	22.48	700.73	186.00	10.10
2019	Yunnan	I	914.54	19.00	7.14	404.80	109.50	5.59

3.2. CMIP6 Model Evaluation

In order to improve the accuracy of precipitation data predicted by CMIP6, this paper uses the Quantile Mapping method to correct the deviation of daily precipitation data under four different scenarios (SSP1-2.6, SSP2-4.5, SSP3-7.0, SSP5-8.5) in the future period (2020–2050) of the four selected climate models. Calculate six extreme precipitation indexes, including PRCPTPT and R10, and compare the calculated results with the measured data of the watershed. Evaluate the adaptability of the corrected model precipitation data to the extreme precipitation simulation of the Lancang-Mekong Basin using four indicators: annual average, standard deviation, relative error, and spatial correlation coefficient.

Considering the "singleness" and "uncertainty" of a single climate model in the simulation process, this paper uses the extreme precipitation indexes of multiple models processed by MME to evaluate the changes of extreme precipitation in the Lancang-Mekong Basin under different scenarios in the future. It can be seen from Table 5 that the multi-year average values of PRCPTOT, R10, R20, and R95p simulated by MME are slightly lower in all four regions, while the multi-year average values of RX5day and SDII simulated are slightly higher in all four regions. From the standard deviation perspective, the standard deviation of the MME simulation for all indexes in four regions is smaller than that of MSWEP, indicating that the dispersion of the extreme precipitation indexes simulated by MME is relatively small. The relative error between the indexes simulated by MME and MSWEP is relatively small, indicating that the simulation effect is very good.

Table 5. Evaluation of simulation ability of extreme precipitation indexes after MME correction.

	Evaluation Index	Annual Average		Standard Deviation		Relative Error/%	Spatial Correlation Coefficient
		MSWEP	MME	MSWEP	MME		
region I	PRCPTOT/mm	635.989	620.492	59.157	36.277	−2.437	0.997
	R10/d	13.597	13.440	2.288	1.342	−1.155	1.000
	R20/d	1.851	1.749	0.827	0.323	−5.511	0.998
	R95p/mm	245.898	241.934	23.663	10.917	−1.612	0.999
	Rx5day/mm	58.693	61.126	7.024	3.563	4.145	0.981
	SDII/(mm/d)	4.813	4.818	0.331	0.158	0.104	0.996
region II	PRCPTOT/mm	1203.847	1193.630	114.533	92.687	−0.849	1.000
	R10/d	39.016	38.785	4.664	4.052	−0.592	1.000
	R20/d	10.857	8.466	2.091	1.311	−22.023	0.999
	R95p/mm	446.406	438.584	36.871	24.241	−1.752	0.999
	Rx5day/mm	106.622	115.534	18.361	8.943	8.359	0.982
	SDII/(mm/d)	7.434	7.461	0.483	0.344	0.363	1.000
region III	PRCPTOT/mm	1513.839	1474.808	129.991	92.136	−2.578	0.997
	R10/d	51.178	50.230	5.796	3.721	−1.852	0.997
	R20/d	16.531	16.289	2.42	1.841	−1.464	0.998
	R95p/mm	574.997	537.052	42.844	27.900	−6.599	0.996
	Rx5day/mm	131.003	146.267	17.659	11.282	11.652	0.978
	SDII/(mm/d)	8.723	8.845	0.499	0.358	1.399	0.994
region IV	PRCPTOT/mm	1703.094	1648.695	144.539	117.210	−3.194	0.998
	R10/d	56.495	55.320	5.273	4.523	−2.080	0.999
	R20/d	20.272	19.669	2.464	2.449	−2.975	0.999
	R95p/mm	615.371	590.117	50.826	40.637	−4.104	0.991
	Rx5day/mm	151.82	167.075	15.084	18.003	10.048	0.964
	SDII/(mm/d)	9.472	9.444	0.487	0.544	−0.296	0.995

In addition, based on the spatial distribution characteristics of each index, this paper analyzes the simulation effect of MME on the extreme precipitation index in the Lancang-Mekong River Basin. As can be seen from Figure 6, MME can well present the spatial distribution characteristics of each extreme precipitation index, that is, precipitation and precipitation intensity gradually increase from the upper reaches to the lower reaches of Lancang-Mekong River Basin. Meanwhile, the simulated extreme precipitation center is also very close to the observed extreme precipitation center. In general, the spatial correlation coefficient between MME and measured data is more than 0.9. Combined with the spatial distribution, it can be seen that MME has a good simulation ability for each extreme precipitation index. In conclusion, MME can well simulate the extreme precipitation indexes in the Lancang-Mekong River basin during 1981–2014. It can be applied to evaluate the characteristics of future changes of the extreme precipitation indexes in the Lancang-Mekong River basin.

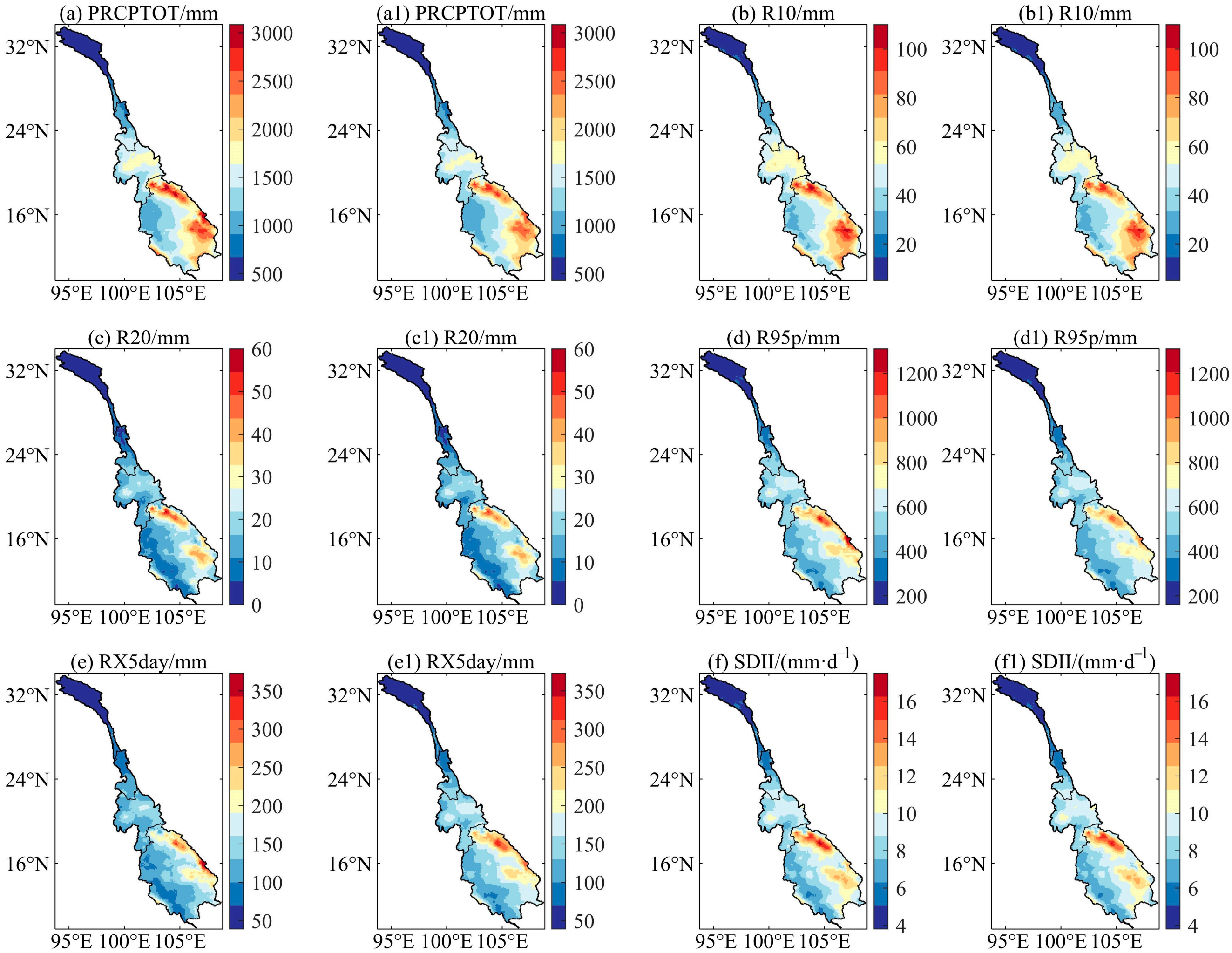

Figure 6. Spatial distribution of extreme precipitation index in Lancang-Mekong River from 1980 to 2014. Note: (**a**–**f**) represents MSWEP data, (**a1**–**f1**) represents historical MME.

3.3. Future Change Projection Based on CMIP6 Simulations

3.3.1. Temporal Variation Characteristics of Extreme Precipitation under Different Scenarios

As shown in the figures (Figures 7 and 8), the extreme precipitation indexes of each sub-regions in the Lancang-Mekong Basin show an upward trend in the future. In region I, except for the RX5day under the SSP1-2.6 scenario and the R10, R20, RX5day, SDII under the SSP5-8.5 scenario, the upward trend is not significant, the change rates of other indexes are significantly increased under each scenario. In the SSP1-2.6 and SSP2-4.5 scenarios of region II, the change rates of most indexes significantly increased, while in the SSP3-7.0 and SSP5-8.5 scenarios, the upward trend of all indexes is not significant. In region III, under the SSP1-2.6 and SSP5-8.5 scenarios, except for R10 under the SSP1-2.6 scenario and PRCPTOT, R10 under the SSP5-8.5 scenario, other indexes show a significant upward trend. However, under the SSP2-4.5 and SSP3-7.0 scenarios, only the R95p and SDII showed a significant upward trend under the SSP3-7.0 scenario, and no significant increase is observed in other indexes. In the SSP5-8.5 scenario of reigon IV, only the upward trend of SDII is not significant, while other indexes increased significantly. In other scenarios, except for the significant upward trend of R20 under the SSP1-2.6 scenario, the upward trend of other indexes is not significant.

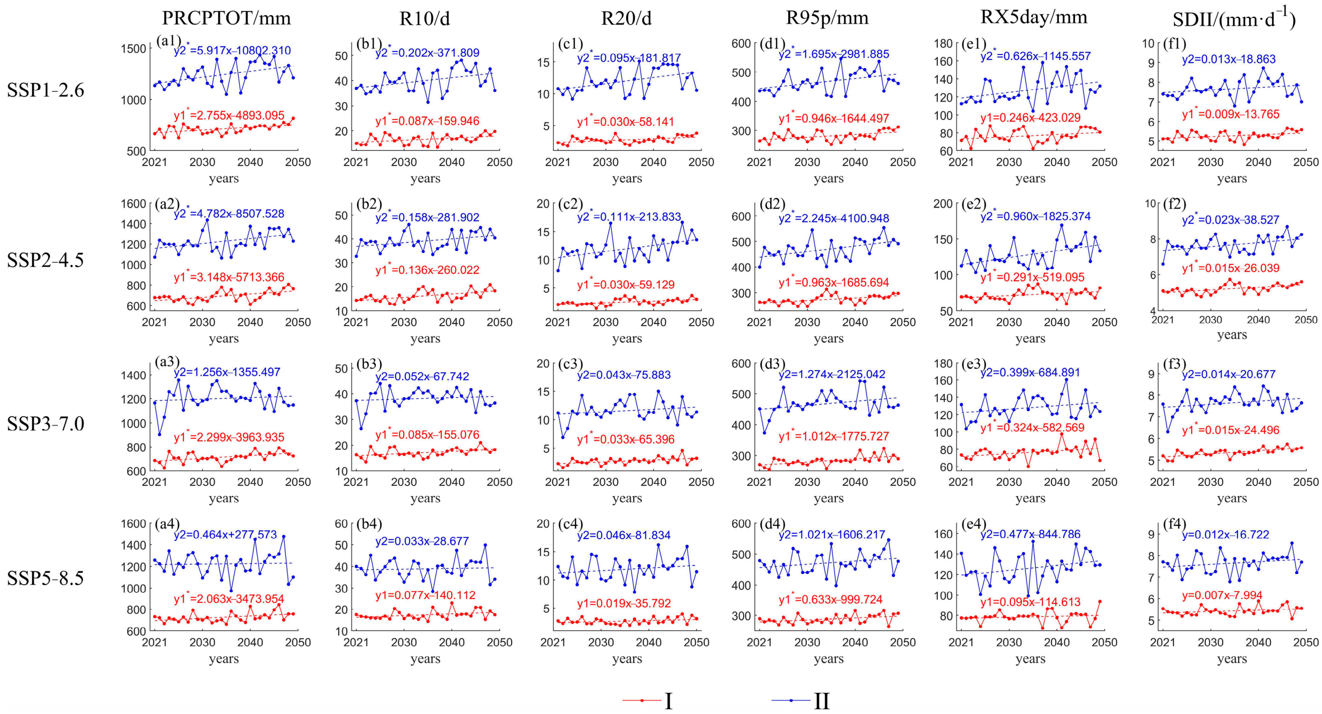

Figure 7. Trends of extreme precipitation indexes under different scenarios in region I and II from 2021 to 2050. Note: * in the figure indicates that it passed the significance test of 0.05.

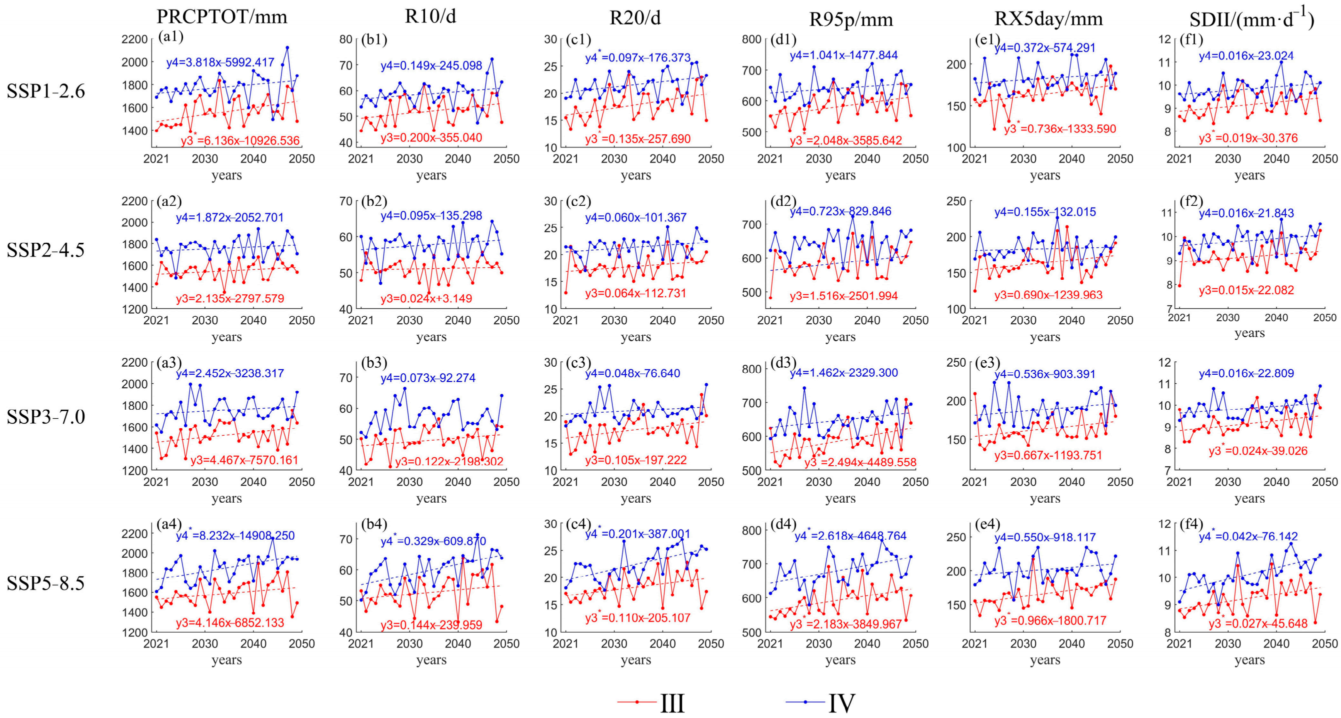

Figure 8. Trends of extreme precipitation indexes under different scenarios in regions III and IV from 2021 to 2050. Note: * in the figure indicates that it passed the significance test of 0.05.

Comparing the annual average of extreme precipitation indexes in the future period with the historical period (Table 6), it can be concluded that: (1) Most indices showed an increasing trend in the future period; only R10 under the SSP2-4.5, SSP3-7.0, and SSP5-8.5 scenarios in region II and the SSP3-7.0 scenario in the region III have a small decrease. (2) From the perspective of each region, in the future, the growth rates of R10 and R20 in region I will be relatively large, increasing by more than 16% and 20%, respectively, compared to the historical period. However, the growth rates of R20 and RX5day in regions II, III, and IV will be relatively large, with the growth rates of the two indexes concentrated between 4–11% and 18–31%, respectively. (3) The magnitude of index changes varies among different regions under four scenarios, with most indexes in regions I, III, and IV showing the largest increase under the SSP5-8.5 scenario and most indexes in region II showing the largest increase under the SSP1-2.6 scenario. The indexes of region I show the smallest increase under the SSP2-4.5 scenario, while the indexes of regions II, III, and IV show a relatively flat increase under the SSP2-4.5 and SSP3-7.0 scenarios. Overall, in any scenario in the future, the Lancang-Mekong Basin will experience stronger extreme precipitation events. Therefore, each region should choose to develop under the scenario of relatively small changes in extreme precipitation index within its own situation to reduce the risk of extreme weather disasters.

Table 6. Changes of extreme precipitation indexes in future period relative to historical period.

	Scenarios	PRCPTOT	R10	R20	R95p	RX5day	SDII
I	SSP1-2.6	9.90%	19.30%	36.92%	12.11%	27.45%	9.26%
	SSP2-4.5	6.83%	16.53%	28.13%	9.74%	20.25%	8.45%
	SSP3-7.0	10.44%	24.08%	41.14%	13.64%	27.05%	11.43%
	SSP5-8.5	11.44%	25.07%	38.10%	15.00%	29.91%	12.52%
II	SSP1-2.6	2.35%	1.64%	8.23%	4.15%	20.07%	2.68%
	SSP2-4.5	0.99%	−0.68%	6.89%	4.31%	19.44%	2.69%
	SSP3-7.0	0.17%	−1.55%	6.92%	4.78%	20.67%	3.24%
	SSP5-8.5	1.02%	−0.75%	7.94%	4.95%	18.63%	2.67%
III	SSP1-2.6	3.82%	2.72%	8.60%	6.49%	25.60%	5.55%
	SSP2-4.5	2.73%	0.38%	8.24%	7.21%	25.75%	5.52%
	SSP3-7.0	1.47%	−1.84%	6.77%	7.89%	25.91%	5.83%
	SSP5-8.5	5.41%	3.81%	11.21%	8.90%	27.86%	6.57%
IV	SSP1-2.6	4.90%	5.13%	6.89%	3.93%	19.38%	4.40%
	SSP2-4.5	3.80%	3.23%	6.11%	4.29%	19.52%	4.28%
	SSP3-7.0	3.32%	2.36%	4.00%	5.03%	23.16%	4.48%
	SSP5-8.5	8.58%	6.78%	10.81%	10.18%	31.59%	7.16%

3.3.2. Spatial Variation Characteristics of Extreme Precipitation under Different Scenarios

Figures 9–12 show the spatial distribution of extreme precipitation indexes change rates in the Lancang-Mekong Basin under different scenarios in the future period. In the region I, the indexes change rates show obvious zonal differentiation. Under the scenarios SSP1-2.6 and SSP3-7.0, from north to south, the change rates of each index show a trend of decreasing–increasing–decreasing, and the maximum value is concentrated in the south-central region, where all indexes show an upward trend. Under the scenario of SSP2-4.5, the change rates of each index show an increasing–decreasing–increasing–decreasing trend from north to south, and the maximum change rates are distributed in the south-central region. Except that the change rates of R10 and SDII tend to be 0 in some parts of the northern and central regions, the change rates of other indexes show an increasing trend in the whole region. In the SSP5-8.5 scenario, R95p and SDII show a decreasing trend from north to south, and the rate of change of R95p in the southern region slightly increases, and the maximum values of the two indexes are in the northern region, while the change regularity of other indexes is the same as that in the SSP1-2.6 scenario.

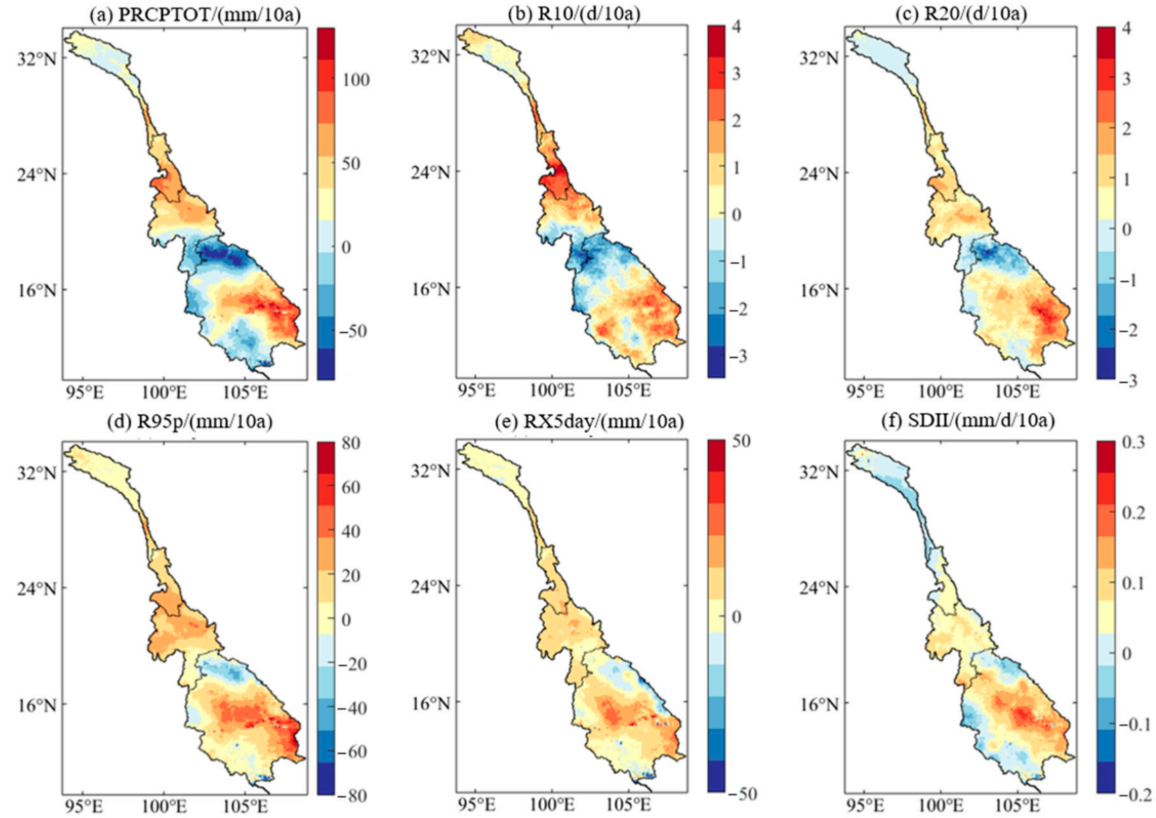

Figure 9. Spatial distribution of extreme precipitation indexes change rates under the SSP1-2.6 scenario.

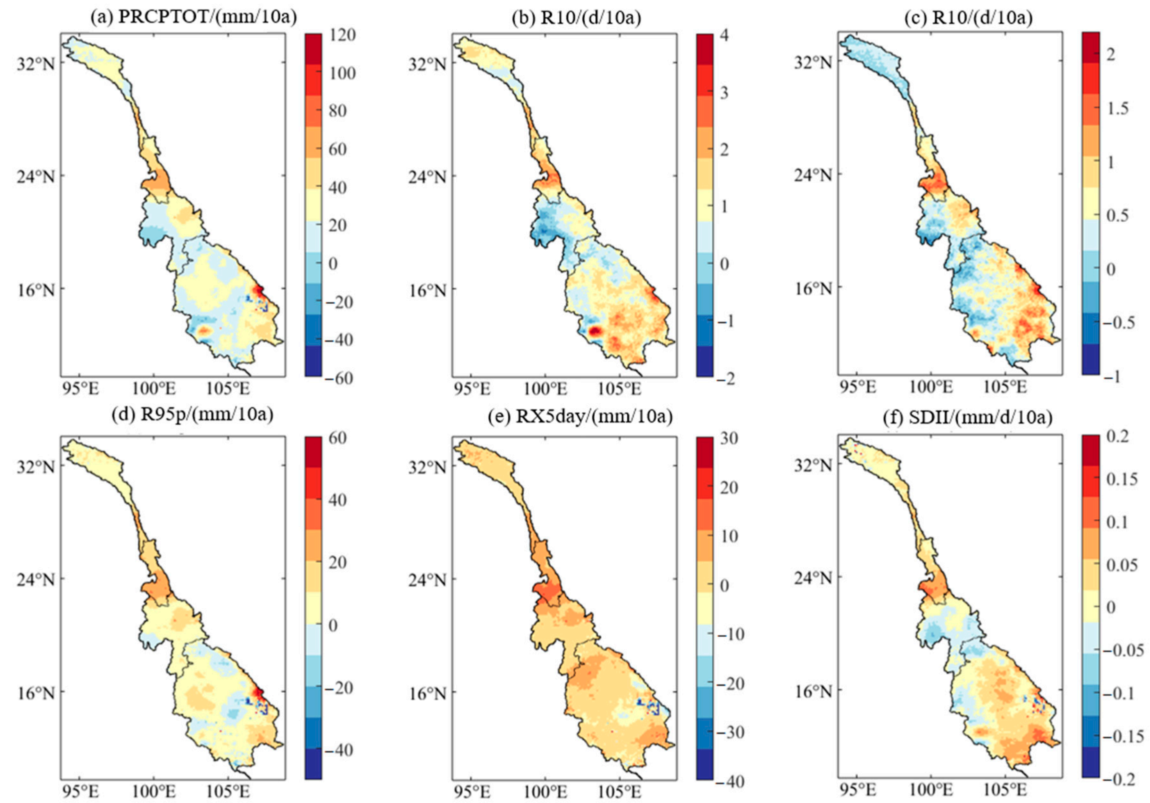

Figure 10. Spatial distribution of extreme precipitation indexes change rates under the SSP2-4.5 scenario.

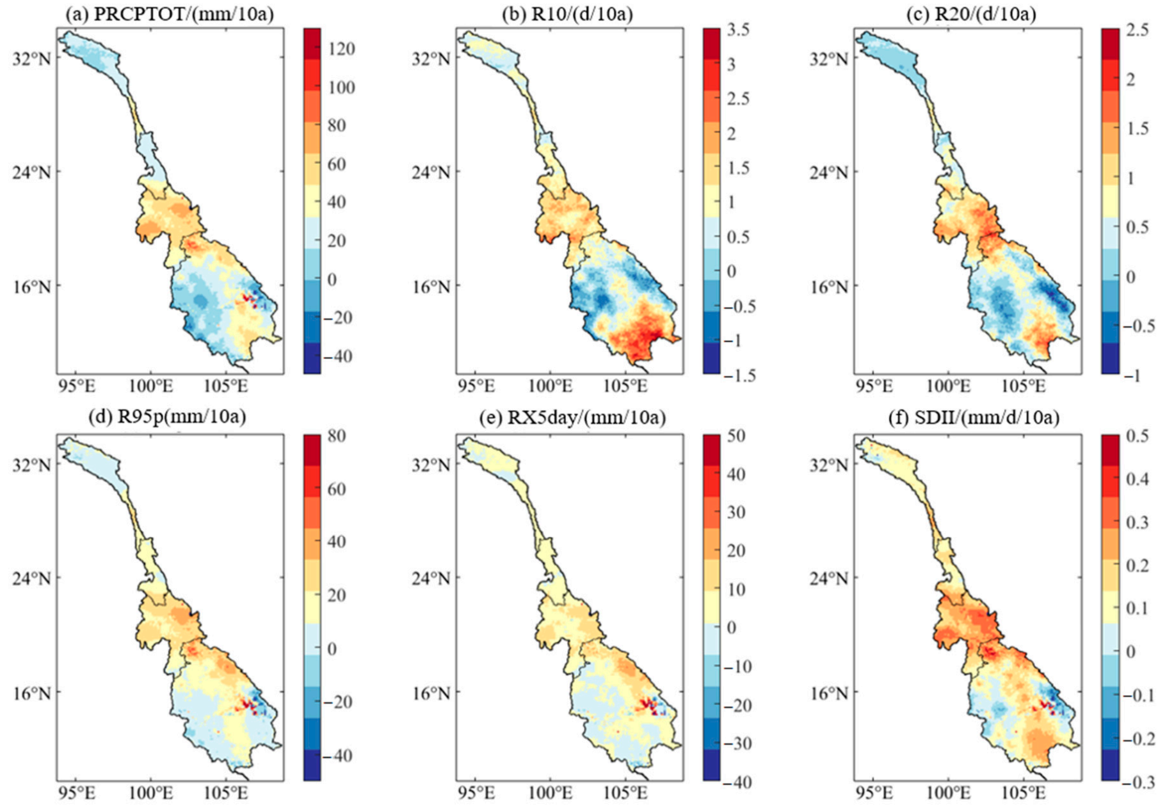

Figure 11. Spatial distribution of extreme precipitation indexes change rates under the SSP3-7.0 scenario.

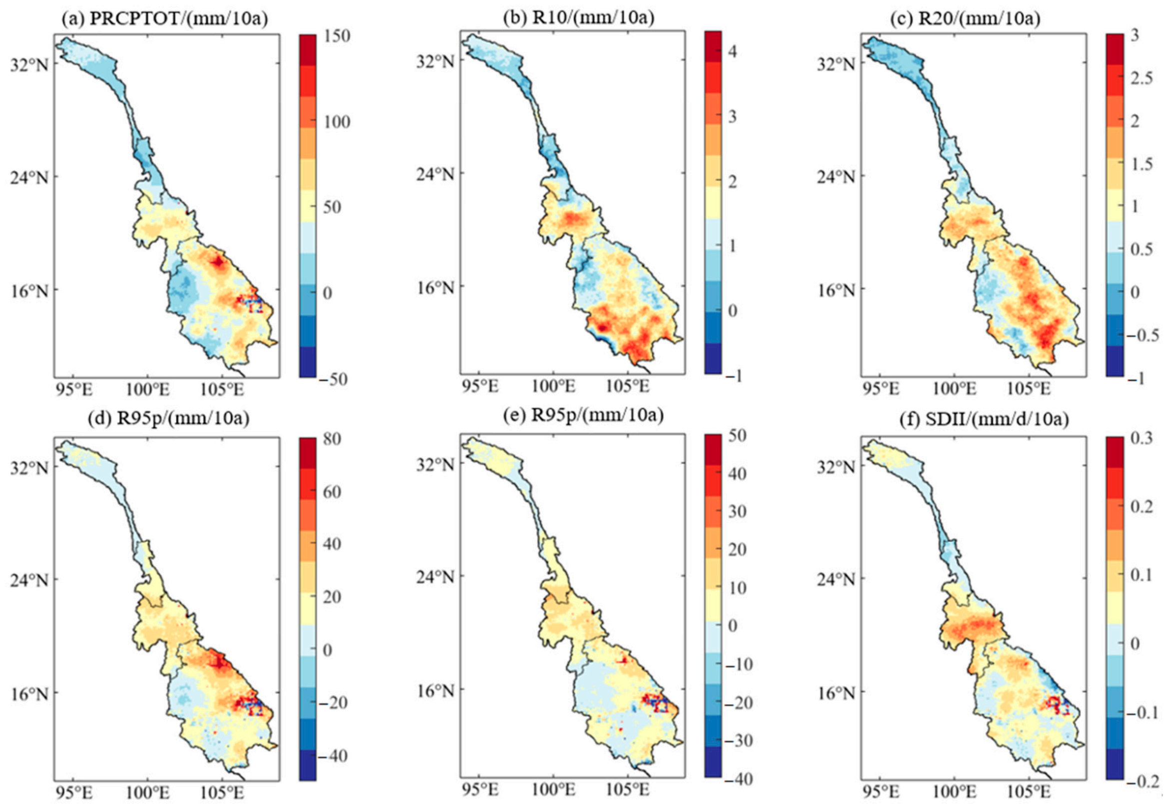

Figure 12. Spatial distribution of extreme precipitation indexes change rates under the 5-8.5 scenario.

In region II, under the scenario of SSP1-2.6, the indexes change rates gradually increase from north to south. Except for R10, the maximum of the index change rate is in the south-central region, the maximum of the other indexes' change rates are concentrated in the southern region. Under the scenario of SSP2-4.5, all the indexes change rates increase first and then decrease from north to south, and the maximum change rates are concentrated in the south-central region. Under SSP3-7.0, the change rate of PRCPTOT increases gradually from north to south, and the change rate of RX5day decreases first and then increases from north to south. In most areas, the change rate of RX5day is concentrated in the range of 0~10 mm/10a, and only in a small part of the central area, the change rate decreases slightly. The change rates of other indexes show a trend of increase–decrease–increase from north to south, and the maximum change rates of all indexes are concentrated in the southern region. Under the scenario of SSP5-8.5, the change trend of each index change rate is mostly the same as that of SSP1-2.6, and the maximum value of each index change rate is concentrated in the southern region.

In region III, the maximum value of the indexes change rates under the four scenarios is concentrated in the central region. The distribution of the maximum value of the indexes change rates under different scenarios is slightly different. In the SSP1-2.6 scenario, except for a small part of the southern region, the indexes' change rates in other regions show an increasing trend, and the maximum value is distributed in the central eastern region. Under the SSP2-4.5 scenario, the maximum distribution of indexes' change rates is the same as SSP1-2.6, with most indexes showing a decrease in change rate in the western region. Under the SSP3-7.0 and SSP5-8.5 scenarios, the indexes' change rates show an increasing trend throughout the entire region. The maximum value of the indexes' change rates under the SSP3-7.0 scenario is distributed on the east and west sides of the central region, while the maximum value of the indexes' change rates under the SSP5-8.5 scenario is distributed in the central region. In all four scenarios, the rates of change of the indexes gradually decreases from the maximum to both ends.

In region IV, under the SSP1-2.6 scenario, the change rate of each index gradually increases from northwest to southeast, and the maximum value is distributed in the central eastern region. Under the SSP2-4.5 scenario, the change rate of the RX5day shows an increasing trend in most regions, with the increase concentrated in 0~10 mm/10a, only slightly decreasing in the central eastern region. The maximum change rate of RX5day is distributed in the northern and southern regions, while the distribution regularities of other indexes is generally the same as under the SSP1-2.6 scenario. In the SSP3-7.0 and SSP5-8.5 scenarios, except for R10 and R20, the maximum value of the other indexes change rates are distributed in the central eastern region, and the change rates in the northern eastern region also increase significantly. The change rates gradually decrease from the central eastern region to the east and west sides, while the maximum value of the R10 and R20 change rate is distributed in the southern region, and their change rates first decrease and then increase from north to south.

Overall, in the future, the central southern area of region I, the central southern area of region II, the central area of region III, and the southeastern area of region IV in the Lancang-Mekong Basin will face stronger extreme precipitation events. Especially in areas I and IV, the increase in extreme precipitation events will lead to more serious consequences. The southern area of region I is the narrowest part of the entire watershed, and extreme precipitation events are more likely to cause disasters such as flash floods and mudslides, causing serious damage to the local ecosystem. The southeast of region IV is a large area of farmland, and a large increase in its index change rate can easily cause crop root hypoxia and death, leading to huge economic losses. Compared with the historical period, except for region III, the maximum distribution of indexes change rates of each region will move southward in the future. In addition, the maximum value of indexes changes rates in the future and the minimum value of indexes change rates in the historical period in regions I, II, and III are all distributed in the same region. However, regions with relatively low index change rates during historical periods often face problems such as insufficient flood control facilities, incomplete warning systems, and weak flood control awareness among residents, which can easily lead to larger disasters when facing sudden extreme precipitation events. Therefore, it is necessary for countries in the Lancang-Mekong Basin to strengthen their prediction and protection against disasters such as heavy rainfall and floods in the future.

3.3.3. Kernel Density Estimation of Extreme Precipitation

Figures 13–16 show the Kernel Density Estimation of extreme precipitation indexes in each region of the Lancang-Mekong Basin. In region I (Figure 13), the six indexes' kernel density curves all move to the right, indicating that the mean extreme precipitation indexes in the region will increase from 2021 to 2050; the amount of precipitation and the number of precipitation days will increase in the future. In the kernel density of extreme precipitation indexes of region II (Figure 14), the position of the kernel density curves of most indexes is not much different from that of the historical period, but the tail end of the kernel density curves mostly extend to the right, which indicates that the mean value of extreme precipitation indexes in the future period are not much different from that of the historical period. However, the increasing probability of medium and high values of each index indicates that the possibility of extreme precipitation events in this region will increase in the future. In the kernel density of extreme precipitation indexes of region III (Figure 15), the kernel density curves of all indexes in the future period move to the right compared with the historical period, it indicates that the mean extreme precipitation indexes in this region will increase in the future period. The tail end of the kernel density curves of R20, R95p, RX5day, and SDII all extend to the right under the four scenarios, indicating that the probability of high values in each index increases. Therefore, the possibility of extreme precipitation events in this region in the future also increase. In the kernel density of extreme precipitation indexes of region IV (Figure 16), the kernel density curves also move to the right, and the amount of precipitation and the number of precipitation days in the future will increase. Under the scenarios of SSP1-2.6, SSP3-7.0, and SSP5-8.5, the tail end of most of the kernel density curves extend to the right. This indicates that the probability of extreme precipitation events will increase in the future. Under the scenarios SSP2-4.5, the tail of kernel density curves of R95p, RX5day, and SDII extend to the right, while the PRCPTOT, R10, and R20 does not. It indicates that under the SSP2-4.5 scenario, the possibility of maximum rainfall in this region is increasing, while the possibility of maximum rainfall days is not increasing. Therefore, in the future, rainfall in this region will be more concentrated, and extreme precipitation events will be more likely to occur.

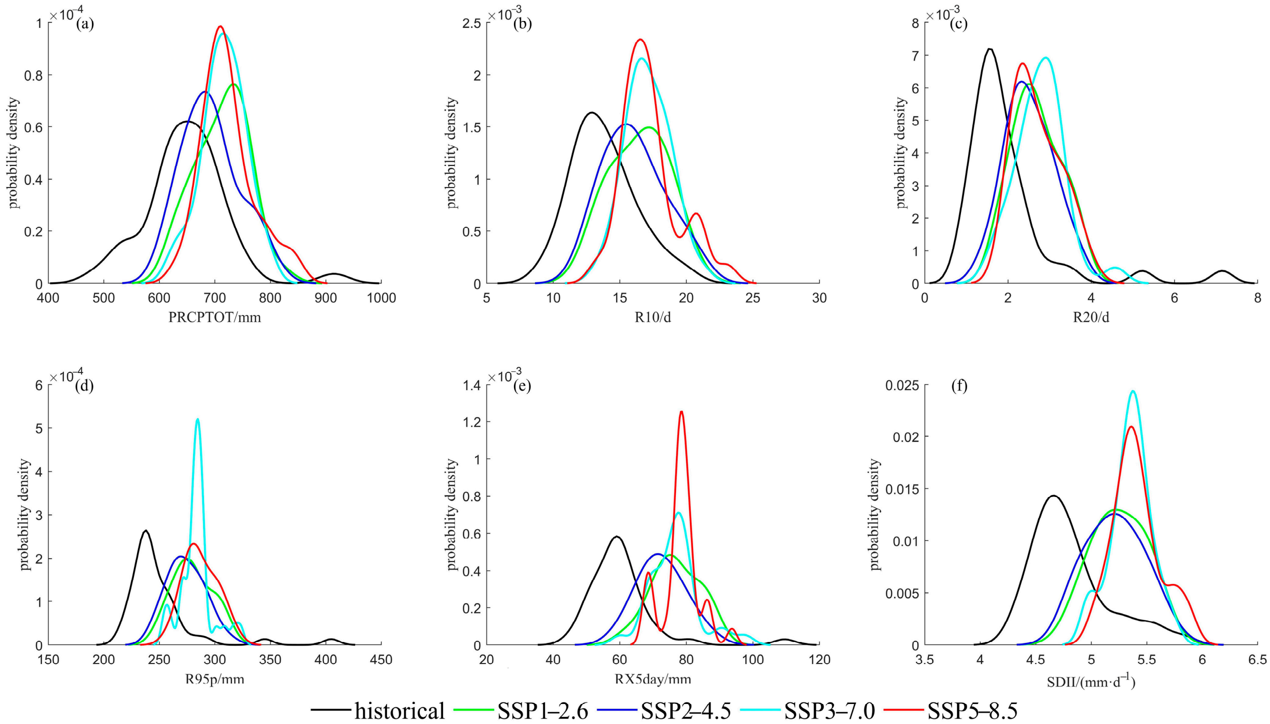

Figure 13. Kernel density estimation of extreme precipitation index in region I.

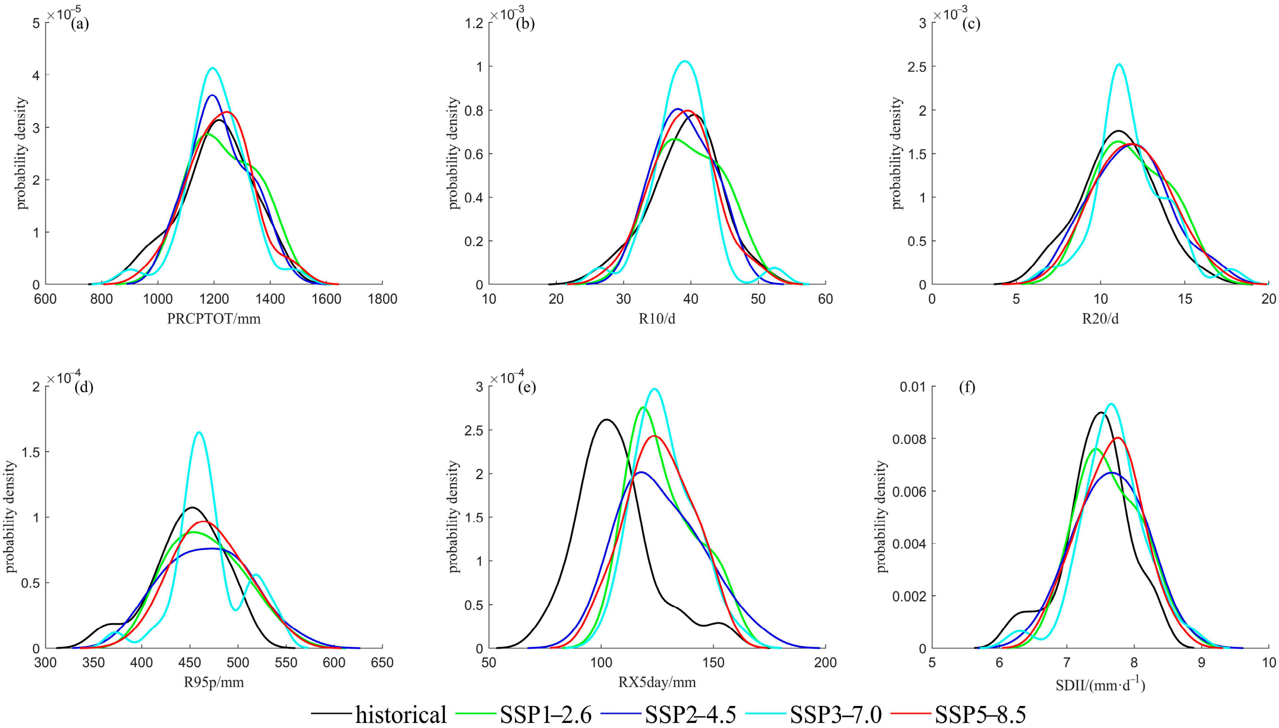

Figure 14. Kernel density estimation of extreme precipitation index in region II.

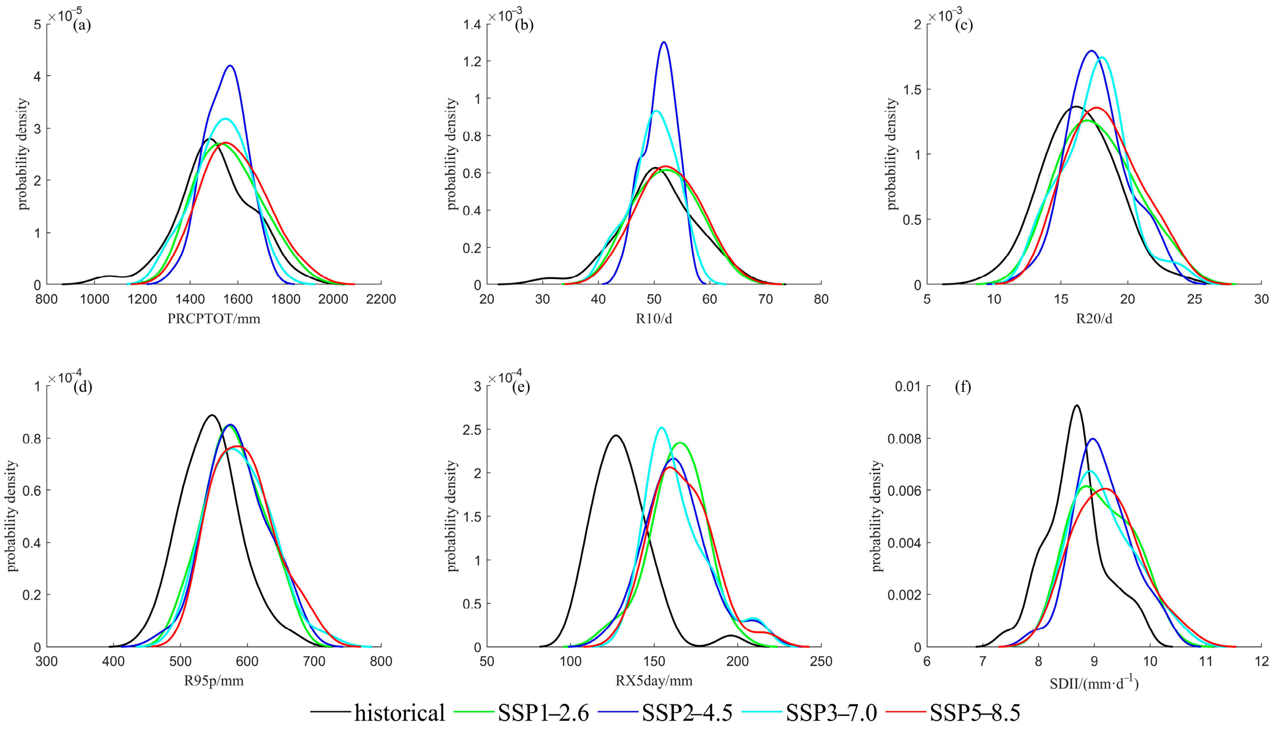

Figure 15. Kernel density estimation of extreme precipitation index in region III.

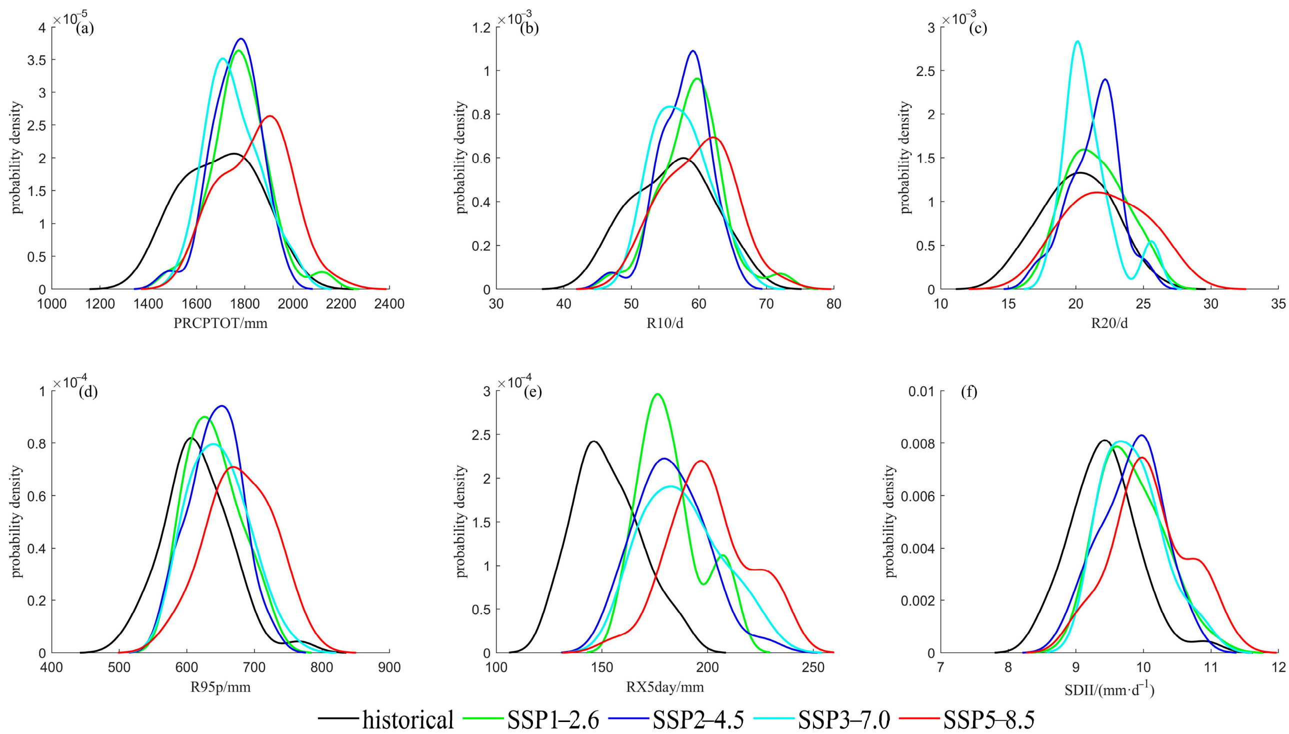

Figure 16. Kernel density estimation of extreme precipitation index in region IV.

4. Discussion

Global warming is currently one of the most important environmental issues, and as temperatures rise, the intensity and frequency of heavy precipitation events will also increase. According to statistics, a total of 61 floods occurred in the Mekong River Basin between 2011 and 2017, resulting in economic losses of approximately $43.5 billion, with an average economic loss of up to $700 million per flood [36]. It has caused huge economic losses and casualties to the countries and people in the river basin. In terms of flood control safety, the intensification of extreme precipitation is likely to cause damage to water conservancy facilities. For example, in July 2018, the dam in Azupo Province in southern Laos failed to cope with a rainstorm, resulting in dam failure, endangering flood control safety. In terms of ecosystem, the central and northern regions of the Lancang-Mekong Basin have large terrain fluctuations, and the increase of precipitation is prone to large-scale soil erosion. The southern part of the Lancang-Mekong River basin is a plain with fertile soil and dense farmland, and the increase of extreme precipitation is prone to cause the anoxic death of vegetation roots, which has an impact on the local ecosystem. In addition, the Lancang-Mekong Basin is an important cross-border river in Southeast Asia. Different countries within the basin are located in different geographical locations and have different demands for water management in the basin. When facing extreme precipitation events, the lack of the same water management concept often leads to insufficient cooperation momentum. The increase in extreme precipitation undoubtedly poses higher requirements for water resource management in cross-border watersheds. Therefore, countries within the basin should accelerate the construction of water conservancy facilities and conduct vulnerability checks on various water conservancy facilities in the future; improve the early warning system and emergency response work after foreseeing dangerous situations, saving time for emergency evacuation; strengthen cooperation among countries within the basin; and establish a joint scheduling mechanism for upstream and downstream reservoirs, in order to better play the role of reservoir scheduling and respond to future flood threats [37].

In addition, this paper analyzed the correlation between six extreme precipitation indices and flood events and predicted the likelihood of future floods based on the trend of index changes. However, this speculation is vague, and the occurrence of flood disasters is also related to the underlying surface. Therefore, analyzing the changes in flood events based on the underlying surface conditions is the next task of this study.

5. Conclusions

This paper uses the extreme precipitation indexes to analyze the precipitation data of different regions in the Lancang-Mekong Basin from 1980 to 2020, and studies its temporal and spatial variation rules. By correcting the deviation of precipitation data of four climate models in CMIP6, the MME of four climate models is used to predict the development trend of extreme precipitation indexes from 2021 to 2050. The following conclusions are drawn:

(1) From 1980 to 2020, extreme precipitation events showed an increasing trend in region I and region IV. In region III and region IV, the extreme precipitation events showed a decreasing trend. Among the four sub-regions, only the SDII in region I experienced a mutation in 2004, indicating that the climate status of Lancang-Mekong River was relatively stable during 1980–2020. Spatially, the maximum values of each index change rate in the historical period were concentrated in the northern part of region I, the middle part of region II, the southern part of region III, and the eastern part of region IV.

(2) In the future, the extreme precipitation indexes in each region of the Lancang-Mekong Basin show an increasing trend. Compared with the annual average value of each index in the historical period, the multi-year average values of most indexes in the future period have increased, indicating that the Lancang-Mekong Basin may experience more intense extreme precipitation events in the future. Spatially, the maximum change rates of extreme precipitation index in each region in the future are the southern part of region I, the central part of region II, the central part of region III and the southeastern part of region IV. Among them, the southern part of region I is the longest and narrowest part of the whole basin, where the increase of extreme precipitation is more likely to cause landslides, debris flows, and other hazards. In regions II, III, and IV, there are large areas of agricultural land, and the increase of extreme precipitation events is easy to cause crop death and hinder economic development. Compared with the historical period, the maximum index change

rate in the future period and the minimum index change rate in the historical period in regions I, II, and III were distributed in the same area. However, the areas with low index change rate in the historical period often have problems such as insufficient flood control facilities, imperfect early warning system, and weak flood control awareness of residents, which are easy to cause greater disasters in the face of sudden extreme precipitation events.

(3) There is a good correlation between extreme precipitation events and flood events, and the increase of extreme precipitation index indicates that the possibility of flood in the basin will increase in the future period. In the future, the increase of extreme precipitation indexes in the Lancang-Mekong Basin will be different under different scenarios. Among them, most of the indexes in regions I, III, and IV have the highest growth rate under the SSP5-8.5 scenario, while most indexes in region II have the highest growth rate under the SSP1-2.6 scenario; the indexes in region I have the smallest increase under the SSP2-4.5 scenario, while the indexes in regions II, III, and IV mostly have a relatively flat increase under the SSP2-4.5 and SSP3-7.0 scenarios. To sum up, the high emission scenario has a more serious impact on extreme precipitation events in the Lancang-Mekong River Basin. In the future, countries in the basin should choose scenarios with smaller index changes in the region according to their own conditions for development, so as to reduce the occurrence of disasters such as rainstorm and flood.

Author Contributions: Conceptualization, Y.L. and X.C.; methodology, J.L. and Y.Z.; software, T.G.; validation, J.L.; resources, L.T.; data curation, J.J. and Y.Z.; writing—original draft, J.L.; writing—review and editing, Y.L. and J.L.; supervision, J.Z., G.W. and Y.L.; funding acquisition, Y.L. All authors have read and agreed to the published version of the manuscript.

Funding: This research was funded by the National Key Research and Development Program of China (2022YFC3201701) and National Natural Science Foundation of China (52079079, U2240203, 92047301, 92047203).

Institutional Review Board Statement: Not applicable.

Informed Consent Statement: Not applicable.

Data Availability Statement: Not applicable.

Conflicts of Interest: The authors declare no conflict of interest.

References

1. Zhao, Y.M.; Qian, C.; Zhang, W.J.; He, D.; Qi, Y.J. Extreme temperature indices in Eurasia in a CMIP6 multi-model ensemble: Evaluation and projection. *Int. J. Climatol. J. R. Meteorol. Soc.* **2021**, *41*, 5368–5385. [CrossRef]
2. Horton, D.E.; Johnson, N.C.; Singh, D.; Swain, D.L.; Rajaratnam, B.; Diffenbaugh, N.H. Contribution of changes in atmospheric circulation patterns to extreme temperature trends. *Nature* **2015**, *522*, 465–469. [CrossRef] [PubMed]
3. Kim, Y.H.; Min, S.K.; Zhang, X.; Zwiers, F.; Alexander, L.V.; Donat, M.G.; Tung, Y.S. Attribution of extreme temperature changes during 1951–2010. *Clim. Dyn.* **2016**, *46*, 1769–1782. [CrossRef]
4. Zhou, T.J.; Chen, Z.M.; Chen, X.L.; Zuo, M.; Jiang, J.; Hu, S. Interpreting IPCC AR6: Future global climate based on projection under scenarios and on near-term information. *Clim. Change Res.* **2021**, *17*, 652–663. [CrossRef]
5. Zhou, B.T.; Qian, J. Changes of weather and climate extremes in the IPCC AR6. *Clim. Change Res.* **2021**, *17*, 713–718. [CrossRef]
6. Jiang, X.F.; Li, L.P.; Zhou, L.B. Progress in the Analysis of Extreme Precipitation Characteristics. *Meteorol. Disaster Reduct. Res.* **2012**, *35*, 1–6. [CrossRef]
7. Wang, Z.F.; Qian, Y.F. Frequency and intensity of extreme precipitation events in China. *Adv. Water Sci.* **2009**, *20*, 1–9. [CrossRef]
8. Kunkel, K.E. North American Trends in Extreme Precipitation. *Nat. Hazards* **2003**, *29*, 291–305. [CrossRef]
9. Ayugi, B.; Dike, V.; Ngoma, H.; Babaousmail, H.; Mumo, R.; Ongoma, V. Future Changes in Precipitation Extremes Over East Africa Based on CMIP6 Projections. *Water* **2021**, *13*, 2358. [CrossRef]
10. Xu, H.W.; Chen, H.P.; Wang, H.J. Future changes in precipitation extremes across China based on CMIP6 models. *Int. J. Climatol. J. R. Meteorol. Soc.* **2021**, *41*, 5368–5385. [CrossRef]
11. Tang, H.X. Resource environment in the Lancang-Mekong River Basin and its sustainable development. *Acta Geogr. Sin.* **1999**, *54*, 101–109.
12. Du, D.B.; Liu, C.L.; Hu, Z.D.; Ma, Y.H. The impact of "Asian Water Tower" change on the geopolitical environment around China. *World Reg. Stud.* **2020**, *29*, 223–231. [CrossRef]
13. Chen, X.R.; Wang, X.Y.; Bai, Y.B. Flood and drought losses in Mekong River basin. *J. Econ. Water Resour.* **2019**, *37*, 54–58. [CrossRef]

14. Chen, X.R.; Wang, X.Y.; Bai, Y.B. Spatial-temporal distribution of flood losses in Mekong River basin countries since 1962. *Sci. Disaster* **2019**, *34*, 113–116. [CrossRef]
15. Wu, D.; Zhao, Y.; Pei, Y.S.; Zhai, J.Q. Variation trends of temperature and precipitation in Lancang-Mekong River Basin during 1980–2009. *J. China Inst. Water Resour. Hydropower Res.* **2011**, *9*, 304–312.
16. Li, B.; Li, L.J.; Li, H.B.; Liang, L.Q.; Li, J.Y.; Liu, Y.M.; Zeng, H.W. Changes in Precipitation Extremes in Lancang River Basin,1960–2005. *Prog. Geogr.* **2011**, *30*, 290–298. [CrossRef]
17. Ding, K.X.; Zhang, L.P.; She, D.X.; Zhang, Q.; Xiang, J.W. Variation of extreme precipitation in Lancang River basin under global warming of 1.5 °C and 2.0 °C. *Clim. Change Res.* **2020**, *16*, 466–479. [CrossRef]
18. Quan, N.T.; Khoi, D.N.; Hoan, N.X.; Phung, N.K.; Dang, T.D. Spatiotemporal Trend Analysis of Precipitation Extremes in Ho Chi Minh City, Vietnam During 1980–2017. *Int. J. Disaster Risk Sci.* **2021**, *12*, 131–146. [CrossRef]
19. Shi, W.L.; Yu, X.Z.; Feng, S.; Liao, W.G. Sudden Change and Variation Trend of Extreme Precipitation in Lancang River Basin during 1960–2010. *Water Resour. Power* **2012**, *30*, 1–5.
20. Beck, H.E.; Van, D.A.; Vincenzo, L.; Jaap, S.; Miralles, D.G.; Brecht, M.; Ad, D.E. MSWEP: 3-hourly 0.25° global gridded precipitation (1979–2015) by merging gauge, satellite, and reanalysis data. *Hydrol. Earth Syst. Sci.* **2017**, *21*, 589–615. [CrossRef]
21. Beck, H.E.; Vergopolan, N.; Pan, M.; Levizzani, V.; Wood, E.F. Global-scale evaluation of 22 precipitation datasets using gauge observations and hydrological modeling. *Hydrol. Earth Syst. Sci.* **2017**, *21*, 6201–6217. [CrossRef]
22. Xiong, J.H.; Guo, J.; Guo, S.L.; Li, N.; Wang, J.; Yin, J.B.; Tang, J.L. Estimating probable maximum precipitation based on multisource data of precipitation in the Lancang-Mekong River basin. *J. Hydroelectr. Eng.* **2022**, *41*, 77–86. [CrossRef]
23. O'Neill, B.C.; Tebaldi, C.; Van Vuuren, D.P.; Eyring, V.; Friedlingstein, P.; Hurtt, G.; Knutti, R.; Kriegler, E.; Lamarque, J.; Lowe, J.; et al. The Scenario Model Intercomparison Project (ScenarioMIP) for CMIP6. *Geosci. Model Dev.* **2016**, *9*, 3461–3482. [CrossRef]
24. Lei, H.J.; Ma, J.P.; Li, H.Y.; Wang, J.; Shao, D.H.; Zhao, H.Y. Bias Correction of Climate Model Precipitation in the Upper Heihe River Basin based on Quantile Mapping Method. *Plateau Meteorol.* **2020**, *39*, 266–279. [CrossRef]
25. Liu, S.; Huang, S.; Huang, Q.; Xie, Y.; Leng, G.; Luan, J.; Song, X.; Wei, X.; Li, X. Identification of the non-stationarity of extreme precipitation events and correlations with large-scale ocean-atmospheric circulation patterns: A case study in the Wei River Basin, China. *J. Hydrol.* **2017**, *548*, 184–195. [CrossRef]
26. Feng, Y.L.; He, Z.H.; Jiao, S.L.; Liu, W. Scenario Prediction of Extreme Precipitation in Guizhou Province Based on CMIP6 Climate Model. *Res. Soil Water Conserv.* **2023**, *30*, 282–290. [CrossRef]
27. Limsakul, A.; Singhruck, P. Long-term trends and variability of total and extreme precipitation in Thailand. *Atmos. Res.* **2016**, *169*, 301–317. [CrossRef]
28. Xiao, W.W.; An, B.; Jia, D. Temporal Variation Characteristics of Extreme Weather Events in Ankang from 1955 to 2017. *Res. Soil Water Conserv.* **2017**, *28*, 212–221. [CrossRef]
29. Ya, R.; Li, N.; Yin, S.; Bao, Y.H. Characteristics of Temporal and Spatial Variation of Extreme Climate Events in Inner Mongolia During the Period 1960–2015. *Res. Soil Water Conserv.* **2020**, *27*, 106–112. [CrossRef]
30. Teegavarapu, R.; Nayak, A. Evaluation of long-term trends in extreme precipitation: Implications of in-filled historical data use for analysis. *J. Hydrol.* **2017**, *550*, 616–634. [CrossRef]
31. Tan, X.; Gan, T.Y.; Shao, D. Effects of persistence and large-scale climate anomalies on trends and change points in extreme precipitation of Canada. *J. Hydrol.* **2017**, *550*, 453–465. [CrossRef]
32. Dike, V.N.; Zhao, H.L.; Kece, F.; Gaby, S.L.; Debashis, N. Evaluation and multimodel projection of seasonal precipitation extremes over central Asia based on CMIP6 simulations. *Int. J. Climatol. J. R. Meteorol. Soc.* **2022**, *42*, 7228–7251. [CrossRef]
33. Xu, C.H.; Xu, Y. The Projection of Temperature and Precipitation over China under RCP Scenarios using a CMIP5 Multi-Model Ensemble. *Atmos. Ocean. Sci. Lett.* **2012**, *5*, 527–533. [CrossRef]
34. Ren, D.; Leslie, M.L.; Lynch, J.M. Trends in Storm-Triggered Landslides over Southern California. *Appl. Meteor. Clim.* **2014**, *53*, 217–233. [CrossRef]
35. Liu, F.X.; Wang, Y.J.; Zhao, J.; Chen, X.; Jiang, T. Characteristics of extreme precipitation changes in the middle and lower reaches of the Yangtze River under global warming scenarios of 1.5 °C and 2.0 °C. *Resour. Environ. Yangtze Basin* **2017**, *26*, 778–788. [CrossRef]
36. Chen, X.R.; Wang, X.Y.; Bai, Y.B. Characteristics of natural disasters in five countries of the Mekong River Basin from 1900 to 2017. *J. China Inst. Water Resour. Hydropower Res.* **2019**, *17*, 7.
37. Tu, S. Lancang-mekong water resources security and cooperation: A development-oriented analysis perspective. *Int. Secur. Stud.* **2021**, *39*, 29. [CrossRef]

Disclaimer/Publisher's Note: The statements, opinions and data contained in all publications are solely those of the individual author(s) and contributor(s) and not of MDPI and/or the editor(s). MDPI and/or the editor(s) disclaim responsibility for any injury to people or property resulting from any ideas, methods, instructions or products referred to in the content.